JOURNAL OF APPLIED ELECTROCHEMISTRY 15 (1985) 335–349

*Mechanistic study of Cl_2 evolution at Ti-supported Co_3O_4 anodes**

R. BOGGIO, A. CARUGATI**, G. LODI***, S. TRASATTI

Department of Physical Chemistry and Electrochemistry, University of Milan, Via Venezian 21, 20133 Milan, Italy

Received 15 March 1984; revised 13 June 1984

Co_3O_4 layers were prepared by thermal decomposition of $Co(NO_3)_2$ at various temperatures in the range 200–500° C on a Ti support with and without an interlayer of RuO_2. Kinetic studies were carried out with and without dissolved Cl_2 at various partial pressures in NaCl solutions of concentration in the range 0.5–5 mol dm^{-3}. The effect of the solution pH was especially investigated. Kinetic measurements were carried out both close to and far from equilibrium. The following parameters were determined: transfer coefficient, Tafel slope, stoichiometric number, reaction orders with respect to Cl^-, H^+ and surface sites, activation energy. The most intriguing feature observed was the retarding effect of acidity on the anodic Cl_2 reaction. This has been ascribed to the complex surface behaviour of oxides in solution. A detailed mechanistic scheme has been proposed and discussed. The stability of the oxide surface was monitored by measuring the voltammetric charge in alkaline solution after sets of experiments.

1. Introduction

Co_3O_4 is an electrode material which arouses great interest in the chlor-alkali industry [1, 2] because of its good electrocatalytic properties, ready availability and low cost. Nevertheless, published studies of chlorine evolution at Co_3O_4-activated Ti anodes are scanty and no detailed mechanistic investigation has been reported thus far [3–6]. The aim of the present work has been to study the mechanism of chlorine evolution from concentrated brines and to elucidate the influence of the temperature of Co_3O_4 formation and the effect of the solution pH.

2. Experimental

Square Ti plates of 1 cm^2 geometric surface and 0.5 mm thickness with a tiny stem in the middle of one of the sides were used as support. These were first sandblasted, then etched in boiling 20% HCl, rinsed with distilled water and wiped with filter paper. The preparation of the Co_3O_4 layer was carried out by thermal decomposition of $Co(NO_3)_2 \cdot 6H_2O$ in air at temperatures ranging from 200 to 500° C [7, 8]. A 0.2 mol dm^{-3} solution of the cobalt salt in isopropanol was brushed onto the two faces of the support (immediately after pre-treatment) and the solvent evaporated at 30–40° C. Samples were then fired in a well-furnace at the selected temperature for 10 min. The deposition of additional layers was continued until the desired amount of Co_3O_4 was deposited (about 1.8 mg cm^{-2} corresponding to *c.* 3 μm nominal thickness of the coating). Finally, the samples were annealed for 2 h at the same temperature.

Two sets of electrodes were prepared. In one set Co_3O_4 was deposited directly onto Ti. In the other set, a thin interlayer of RuO_2, prepared at 400° C in the usual way [9], was placed between the Ti and the active layer of Co_3O_4. Layers were prepared at 200, 230, 260, 300, 400 and 500° C. Two samples were prepared at each temperature in each set (total of 24 electrodes). The physicochemical characterization of films of Co_3O_4 on Ti has been reported previously [8].

* Paper presented at the 34th Meeting of the International Society of Electrochemistry, Erlangen, 19–23 September, 1983.

** *Present address*: Assoreni, San Donato Milanese, Milan, Italy.

*** *Permanent address*: Chemical Institute, University of Ferrara, Ferrara, Italy.

0021-891X/85 $03.00 + .12

Solutions for kinetic experiments were prepared volumetrically with double-distilled water. Chemicals (Merck) and gases (SIAD) were used without further purification. Potentials were measured against a saturated calomel electrode, except when ClO_4^- ions were present in solution. In that case, a saturated NaCl calomel electrode was used. Electrodes were placed in a cylindrical cell with a Luggin capillary (connected to the compartment of the reference electrode and coming up from the bottom of the cell) placed at about 1 mm from the lower edge of the plate electrode. Two platinized Pt counter-electrodes facing the two opposite sides of the plate were separated by glass frits from the main compartment. During experiments the solution was usually saturated with pure nitrogen or nitrogen–chlorine mixtures and stirred by a magnetic stirrer. All experiments were carried out at 25 ± 0.1° C unless otherwise stated.

Voltammetric curves were normally recorded in 1 mol dm^{-3} KOH solutions at 20 mV s^{-1} over an anodic potential range of 600 mV starting from − 110 mV (SCE) corresponding to the average rest potential of Co_3O_4 electrodes in the alkaline solution. Voltammetric curves were integrated up to the potential of incipient oxygen evolution and the total charge (anodic + cathodic), henceforth denoted by q^*, has been used as a parameter to characterize the 'electrochemically active' surface area. Details of the determination of q^* will be given in a forthcoming paper [10].

Experiments on chlorine evolution were carried out in 0.5–5 mol dm^{-3} NaCl solutions to which 10^{-2} mol dm^{-3} HCl was added to keep the pH low. The nominal pH of these solutions is *c.* 2 but the effect of the NaCl concentration on the pH value will be discussed later. Potentiostatic curves were started either at the equilibrium potential (in Cl_2 saturated solutions) or at 900 mV (SCE) after a conditioning time of 10 min. The potential was then increased in 20 mV steps and the current was read after 3 min. These experiments were carried out with the aid of a 551 AMEL potentiostat-galvanostat coupled with a 566 AMEL function generator. Currents were either read with a Microva AL 4 Kipp-Zonen galvanometer or recorded with a 862/D AMEL *X–Y* recorder. Potentials were read either with a 667/RM AMEL electrometer or with a 8687 L&N potentiometer. The pH of the solution was measured by means of a 335 AMEL digital pH meter equipped with combined electrodes. These were carefully calibrated before each run using fresh buffers.

Since the electrode surface may undergo modifications upon prolonged anodic polarization, reaction order measurements were carried out by polarizing the electrode only at the selected potential. Thus, the electrode was conditioned for 10 min at 0.9 V (SCE), the potential was then stepped to the selected value and the current read after 3 min. The electrode was then stepped back to the conditioning potential, kept there for 10 min and removed from the cell. This operation was repeated for each different concentration of the species under study.

3. Results and discussion

3.1. Voltametric curves

Fig. 1 shows a comparison between the behaviour of Co_3O_4 in the absence and in the presence of chloride ions. The voltametric curve in the blank solution does not show the typical current maxima related to the adsorption–desorption of oxygenated species [7, 10–12]. This is because this maximum, visible in KOH solutions prior to O_2 evolution, shifts with pH at a greater rate than the anodic process itself [7, 11, 12]. Cl_2 evolution, at the same pH, commences about 140 mV earlier than O_2 evolution. Both curves are featureless prior to the anodic reaction. The charging current is depressed by the presence of Cl^- ions in solution. This may be related to a lowering of the (pseudo) capacitance of the oxide–solution interface as a result of Cl^- adsorption. In fact, the surface of Co_3O_4 at low pHs carries a strong positive charge [13].

3.2. Equilibrium potential

Fig. 2 shows the dependence of the equilibrium potential of Co_3O_4 electrodes on the Cl_2 partial pressure and the Cl^- activity in solution. A strictly Nernstian behaviour is observed at variable p_{Cl_2}, and also at constant a_{Cl^-} in the low Cl_2 pressure range. Small deviations are observed in the high p_{Cl_2} range as a_{Cl^-} is varied. The origin of these small deviations is not clear. Equilibrium poten-

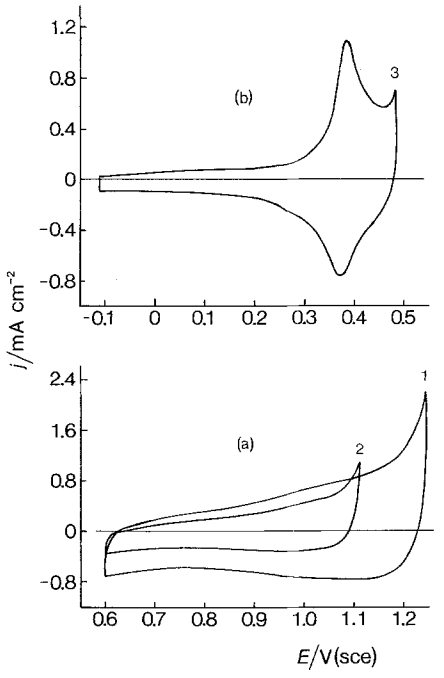

Fig. 1. Typical voltametric curves at 20 mV s^{-1} of Co_3O_4 electrodes (with RuO_2 interlayer) in (a) acidic and (b) basic solutions. 1. 1 mol dm^{-3} $NaClO_4$ + 0.01 mol dm^{-3} $HClO_4$; 2. 5 mol dm^{-3} NaCl + 0.01 mol dm^{-3} HCl; 3. 1 mol dm^{-3} KOH. Temperature of preparation: (a) 230° C; (b) 300° C.

tials were also measured at variable pH between 1 and 3. No dependence of E on pH was observed in the low p_{Cl_2} range which indicates that no mixed potential is appreciably operative in these conditions. In the high p_{Cl_2} range small effects were observed at the lowest Cl^- concentrations. Cl_2 hydrolysis may perhaps have some effect at high Cl_2 pressure and low Cl^- concentration. The (possible) dissolution of the oxide [14] plays, however, a minor role in the range of low Cl_2 overpotential.

Measured potentials are systematically higher by *c.* 4 mV in the region where Nernstian response is observed than those calculated from tabulated E^0 and a_{Cl^-} data [15], most of the difference being presumably related to the unknown value of the liquid junction potential. The highest difference in the region where deviation from the Nernst slope is observed does not exceed 8 mV. Therefore, in the analysis which follows, thermdynamic reversible behaviour will be assumed throughout between 1 and 3. No dependence of E on pH was observed which indicates that no mixed potential is operative in this pH range at Co_3O_4 surfaces. The (possible) dissolution of the oxide [15] therefore plays a minor role in the range of low Cl_2 overpotentials.

3.3. Kinetic measurements close to equilibrium

Fig. 3 shows a typical polarization resistance determination around the equilibrium potential. The reversibility and reproducibility are very satisfactory although small hysteresis effects can be occasionally observed. This may be due to a small drift of the solution pH if Cl_2 hydrolysis is allowed to proceed for too long a time.

The apparent exchange current was derived from the slope of the straight lines such as that in Fig. 3:

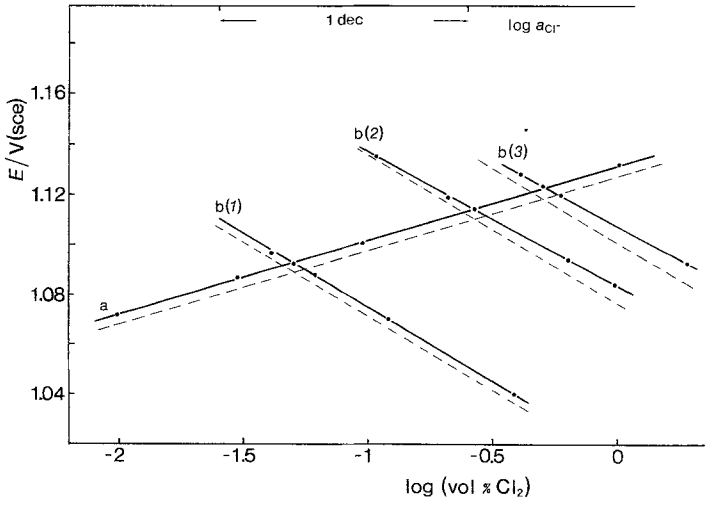

Fig. 2. Equilibrium potentials of Co_3O_4 electrodes in Cl_2 saturated solutions of NaCl + 0.01 mol dm^{-3} HCl: (a) at constant NaCl concentration (1 mol dm^{-3}) and variable Cl_2 partial pressure; (b) at constant gaseous composition 1. 4.98, 2. 26.2, 3. 49.9 vol% Cl_2 + N_2, and variable Cl^- activity. Solid lines: experimental data. Dashed lines: calculated by the Nernst equation with $E^0 = 1.358$ V (NHE) and $E = 0.241$ V (NHE) for the saturated calomel electrode.

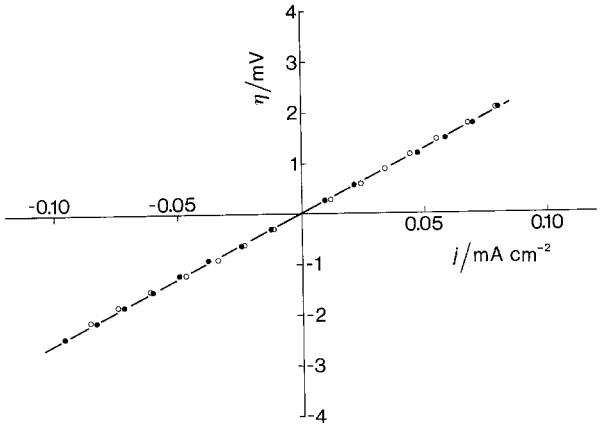

Fig. 3. Typical j–η relationship around the equilibrium potential for a Co_3O_4 electrode (260° C, with RuO_2 interlayer) in a 1 mol dm^{-3} NaCl + 0.01 mol dm^{-3} HCl solution saturated with pure Cl_2 gas. Different symbols indicate different runs (○ – forward and • – backward).

$$(j_0/\nu) = (RT/nF)(\mathrm{d}j/\mathrm{d}\eta) \qquad (1)$$

Fig. 4 shows a typical plot of (j_0/ν) as a function of Cl_2 partial pressure (Cl_2 is assumed to behave ideally). The dashed lines mark the slope equal to 0.5. Although for some electrodes, especially the more active ones (namely, those prepared at low calcination temperatures) the point for the lowest Cl_2 pressure falls somewhat far from the straight line, the experimental data can be taken to conform to a linear dependence. Since:

$$(\mathrm{d}\log j_0/\mathrm{d}\log p_{Cl_2})_{\mu_{Cl^-},T} = \alpha \qquad (2)$$

it follows from Fig. 4 that the anodic transfer coefficient (α) is very close to 0.5.

With the aim of determining the cathodic transfer coefficient independently, the apparent exchange current is plotted in Fig. 5 against the Cl^- activity at constant chlorine pressure. The striking feature of the resulting plot is not its nonlinearity but rather its negative slope throughout. Since the equilibrium potential is governed by the overall reaction:

$$2Cl^- \rightleftarrows Cl_2 + 2e \qquad (3)$$

as inferred from the Nernstian behaviour, the

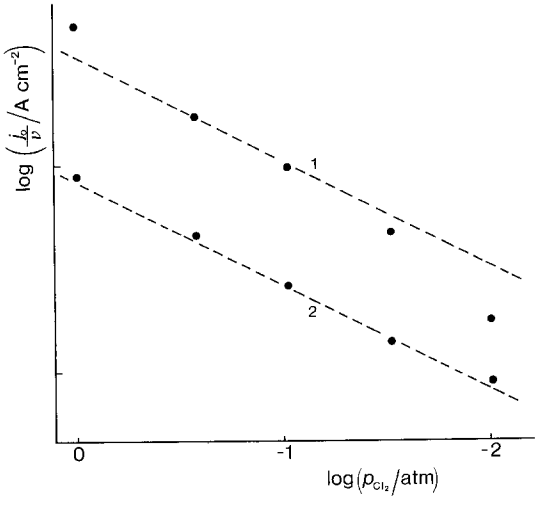

Fig. 4. Apparent exchange current obtained from plots such as Fig. 3 as a function of Cl_2 partial pressure for two Co_3O_4 electrodes. 1. 260° C, with RuO_2 interlayer; 2. 400° C. (– – – – –) Relationship expected for $\alpha = 0.5$.

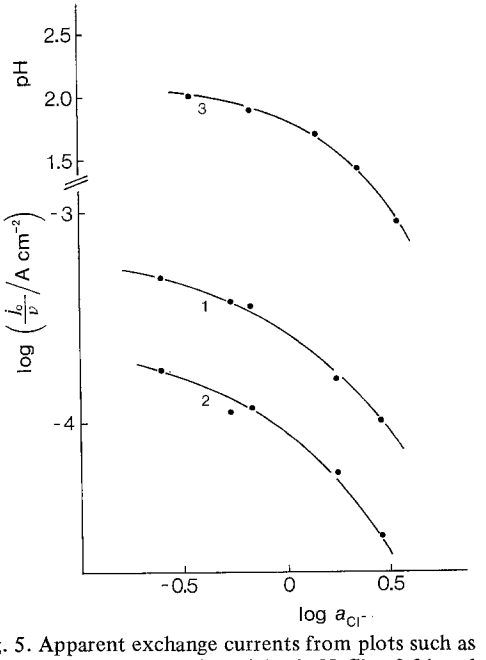

Fig. 5. Apparent exchange currents from plots such as Fig. 3 as a function of Cl^- activity in NaCl + 0.01 mol dm^{-3} HCl solutions for two Co_3O_4 electrodes. 1. 260° C; 2. 500° C, with RuO_2 interlayer. Curve 3 shows the variation of the actual pH of the solutions as a function of NaCl concentration.

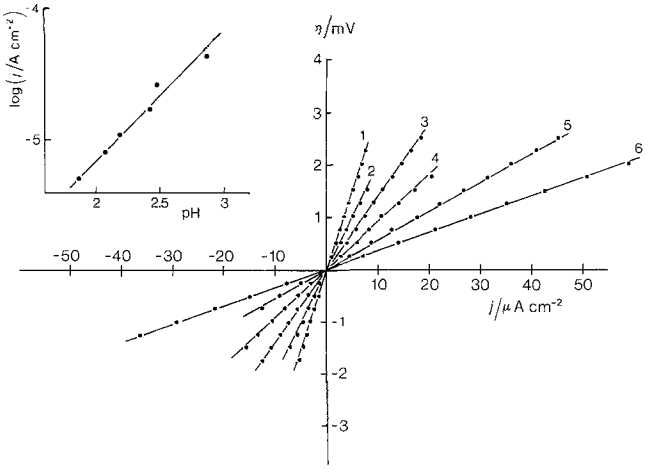

Fig. 6. Variation of the $j-\eta$ relationship around the equilibrium potential for a Co_3O_4 electrode (400° C) in 1 mol dm^{-3} NaCl solutions at different pH saturated with 9.42 vol% Cl_2 + N_2 gas. Equilibrium pH value: 1. 1.87; 2. 2.08; 3. 2.19; 4. 2.42; 5. 2.48; 6. 2.86. Inset: current density at $\eta = 3$ mV as a function of solution pH.

exchange current should depend on Cl^- activity as follows:

$$(\mathrm{d} \log j_0/\mathrm{d} \log a_{Cl^-})_{T,\mu_{Cl_2}} = (x - 2\alpha) \quad (4)$$

where x is the reaction order with respect to Cl^-. Negative slopes can be obtained only if x is less than 1 which seems unlikely.

A clue to the understanding of this outcome can be found in the effect of pH. In principle, the pH should have nothing to do with the Cl_2 equilibrium (provided the conditions are such as to minimize Cl_2 hydrolysis effects, i.e. pH < 4–5) [16]. However, the solution pH shifts with increasing Cl^- concentration as shown by Curve 3 in Fig. 5. This curve strikingly parallels the other two plots. Moreover, in a specific experiment, it was discovered that the apparent exchange current was markedly dependent on pH. This is clearly illustrated by Fig. 6. As shown in the inset, if the current at constant overpotential (recall that E_{rev} does not depend on pH) is plotted as a function of pH, a slope of about − 1 is found which means that H^+ has a retarding effect on Cl_2 evolution. This observation has never been reported before in the literature*.

Since in Fig. 5 the exchange current appears to be entirely dominated by the pH shift, j_0 is very likely to be independent of the Cl^- activity. Therefore $x \simeq 1$ in Equation 3 and the expression of the exchange current can be written as follows:

$$j_0 = nFk^0 a^{\alpha}_{Cl_2} a^{(1-2\alpha)}_{Cl^-} a^{-1}_{H^+} \quad (5)$$

where k^0 is the standard rate constant. Therefore:

$$(\mathrm{d} \log j_0/\mathrm{d} \log a_{Cl^-})_{\mu_{Cl_2},T} = (1 - 2\alpha) + (\mathrm{d\,pH}/\mathrm{d} \log Cl^-) \quad (6)$$

Since in the explored concentration range, the second term on the left-hand side of Equation 6 is negative and $(1 - 2\alpha) = 0$ with $\alpha = 0.5$, the slopes of the curves in Fig. 5 turn out to be negative. Thus the reaction of Cl_2 at Co_3O_4 anodes is thermodynamically independent of but kinetically dependent on the pH.

The effect of the 'electrochemically active surface area' is illustrated in Fig. 7. The points actually gather around a straight line of unit slope. The meaning of this result depends on the physical significance of q^*. Since q^* is largely determined by the anodic current peak prior to O_2 evolution, the straight line in Fig. 7 suggests that Cl_2 evolution takes place at the sites which are active in the adsorption of oxygenated species too. Should q^* measure the total surface area exposed to the solution and Cl_2 evolution occur only at some specific sites whose surface concentration were an exponential function of the surface area, no linear correlation of unit slope would be observed. The same would be the case if the nature of the sites changed with surface concentration. Therefore, either (a) the surface concentration of active sites is directly proportional to the surface area and q^* measures the latter, or (b) q^* measures only the active surface area and no change in the nature of the surface sites occurs with the calcination temperature.

* The effect of pH on Cl_2 evolution was first reported by Krishtalik for RuO_2 and $NiCo_2O_4$ electrodes at a Symposium on Electrocatalysis in Neunkirchen, 14–16 September, 1983 (cf. Krishtalik *et al.* [17]).

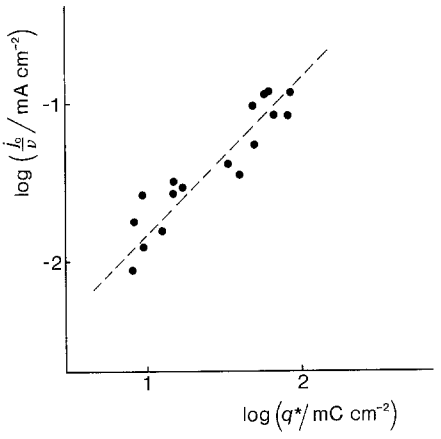

Fig. 7. Apparent exchange current from plots such as Fig. 3 as a function of the voltametric charge, q^*. – – – – – – Straight line of unit slope.

3.4. *Kinetic measurements far from equilibrium*

Fig. 8 illustrates the role played by the RuO_2 interlayer. The experimental data have been corrected for the back reaction [18] and for the *IR drop in solution.* In fact, the latter correction was carried out by means of the current interruption technique using a Pt electrode in place of the Co_3O_4 electrodes. This approach enables one to give evidence of any IR drop in the electrode. Fig. 8 shows that a single Tafel line of 0.040 V is observed up to 0.1 A cm^{-2} (higher current densities have not been explored but there is evidence that nothing different happens there) if a RuO_2 interlayer is present between Ti and Co_3O_4. If RuO_2 is not present, deviations from the Tafel line are observed already at 1 mA cm^{-2}. This is clearly due to a TiO_2 layer which, however thin, shows no miscibility with Co_3O_4 [19] and therefore retains its largely insulating properties.

'True' exchange currents were obtained by back extrapolation of Tafel lines such as that in Fig. 8. By comparing 'apparent' and 'true' exchange currents the stoichiometric number could be obtained:

$$(j_0)_{\text{true}}/(j_0)_{\text{apparent}} = \nu \qquad (7)$$

Fig. 9 shows a graphical analysis of ν as a function of q^*. Out of 15 electrodes 11 gives a value of ν between 1 and 1.1. The mean value is 1.18 which can reasonably be taken as 1 in view of the crucial inaccuracy of the extrapolation procedure (uncorrected *IR* drops tend to increase the resulting value of ν). It is to be noted that there is no significant systematic dependence of ν on q^*.

In Fig. 10 the activity of Co_3O_4 electrodes is compared with that of an RuO_2 electrode [20]. Comparison is made with due attention to the value of q^*, but it is clear that the same physical significance cannot be attached unambiguously to the same value of q^* for the two oxides. Comparison shows that the Tafel slope is the same (0.040 V) but Co_3O_4 electrodes are always less active even for higher q^* values. The results shown above warn that meaningful comparison is possible only if the solution pH is the same.

The Tafel slope is graphically analysed as a function of q^* in Fig. 11. Values derived from

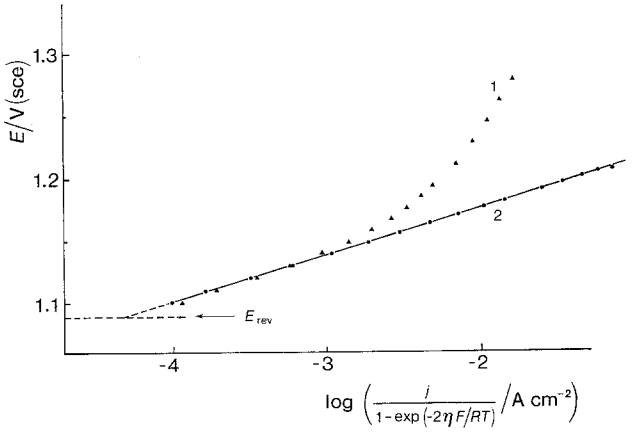

Fig. 8. η–log j relationship (corrected for the back reaction) for two Co_3O_4 electrodes prepared at 260° C: 1. *without* RuO_2 interlayer; 2. *with* RuO_2 interlayer. 1 mol dm^{-3} NaCl solution saturated with 4.98 vol% Cl_2 + N_2 gas. Overpotentials corrected for the *solution* ohmic drop. ——— – Tafel slope of 0.0395 V.

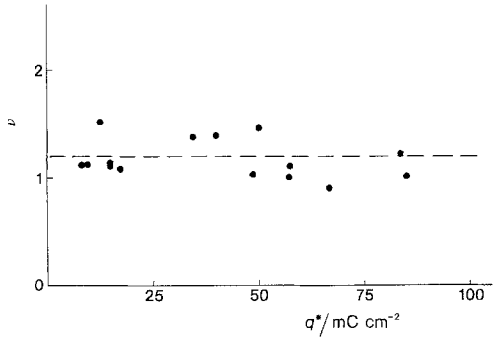

Fig. 9. Stoichiometric number for the chlorine evolution reaction, obtained from the ratio between the true exchange current extrapolated from plots such as Fig. 6 and the apparent exchange current from plots such as Fig. 3, as a function of the voltametric charge, q^*.

polarization data both in the absence and in the presence of Cl_2 dissolved in solution are reported†. The most probable value is 0.040 ± 3 mV and no systematic variation with q^* can be seen. Worthy of mention are the lower Tafel slope for the electrodes with very high value of q^*. The significance of lower Tafel slope values for very active electrodes has been recently illustrated by Losev [21]. Apparent overcorrections of the *IR* drop which should be in fact related to Cl_2 diffusion [22] and saturation problems were actually observed in this work with the most active electrodes. An example is shown in Fig. 10.

3.5. Effect of electrode morphology

Fig. 12 illustrates the general relationship between the electrocatalytic activity and the calcination temperature used to prepare the Co_3O_4 layers. The role of the RuO_2 interlayer does not appear to be crucial in this context. The decrease in activity as T increases parallels the observed decrease in the BET surface area [8]. The small rise in activity at the higher temperatures may be related to some underlayer effect (Co_3O_4 on pure Ti does not work at 500° C owing to very large ohmic drop effects).

It has been suggested [6] that the activity of Co_3O_4, once corrected for surface roughness, still depends on the number of point defects in the lattice (metal vacancies balanced by Co^{3+} in place of some Co^{2+} sites). It is difficult in this work to disentangle the two effects if they are both present. It is however worth mentioning that the value of x in $Co_{3-x}O_4$ is usually determined gravimetrically at the given temperature [23]. Co_3O_4 can, however, release and take up oxygen again reversibly [24, 25] and this must be especially true at the surface. In another work [26], we have found that the point of zero charge of Co_3O_4 does not depend on the calcination temperature. Should the surface stoichiometry depend on this parameter, the variable nature of the surface

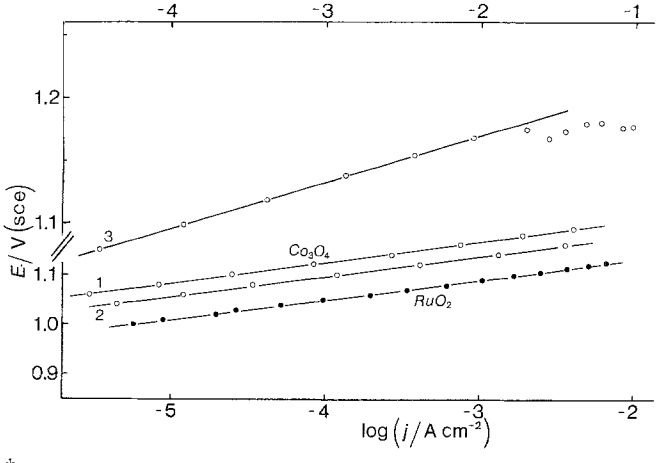

Fig. 10. Comparison of the activity of a Ti/RuO_2 electrode (300° C, $q^* = c.$ 5 mC cm^{-2}) with the activity of two Co_3O_4 electrodes for Cl_2 evolution from N_2 saturated 5 mol dm^{-3} NaCl + 0.01 mol dm^{-3} HCl solutions. 1. 400° C, $q^* = c.$ 5 mC cm^{-2}; 2. 230° C, with a RuO_2 interlayer, $q^* = c.$ 75 mC cm^{-2}. 3. As for line 2 but in the higher potential range. Potentials corrected for the *solution* ohmic drop. ——— – Tafel slopes of 0.00395 V.

† It is to be noted that Tafel lines in the absence and in the presence of Cl_2 dissolved in solution match perfectly. Therefore, the reaction order with respect to Cl_2 is zero.

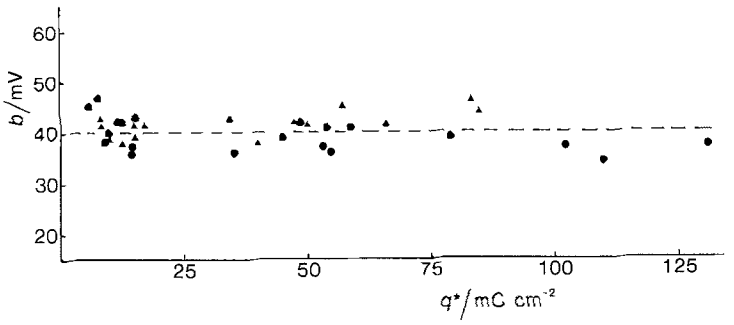

Fig. 11. Dependence of the Tafel slope for Cl_2 evolution on the voltametric charge, q^*, of Co_3O_4 electrodes. • – N_2 saturated 5 mol dm^{-3} NaCl solutions; ▲ – 1 mol dm^{-3} NaCl solutions saturated with 4.98 vol% Cl_2.

would show up through the point of zero charge. Therefore, this particular point deserves further careful study.

The effect of the electrode morphology shows up clearly in Fig. 13 where the electrocatalytic activity at two Cl^- concentrations is plotted as a function of q^*. While in Fig. 13a the experimental points are grouped around a straight line of unit slope, deviation from this behaviour is observed in solution at a lower Cl^- concentration. This outcome can be understood in terms of porosity of the active layer. The supply of Cl^- ions to the inner surface in pores is increasingly difficult as the Cl^- concentration decreases. Under similar circumstances only part of the inner surface works, hence the electrocatalytic activity appears to decrease.

Porosity effects with Co_3O_4 electrodes are, however, of minor importance. In concentrated brine they are not observed. Much more striking results have been reported [20, 27] for RuO_2 electrodes. In that case porosity effects smooth down electrocatalytic activity differences even in 5 mol dm^{-3} NaCl solutions.

3.6. *Activation energy*

The activation energy, $E^{\neq}$, is a kinetic parameter

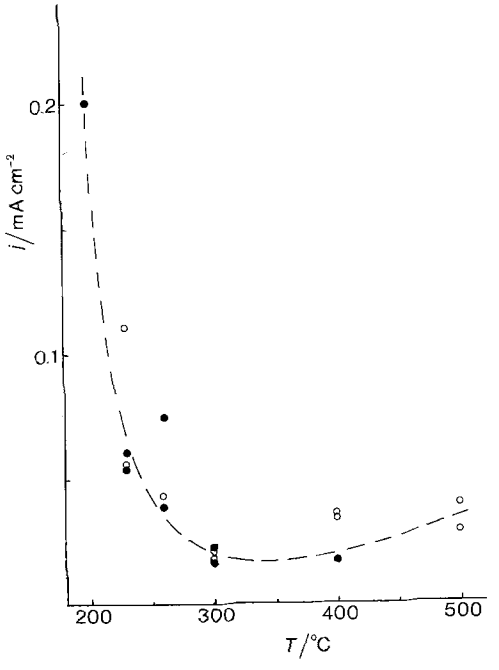

Fig. 12. Variation of the electrocatalytic activity of Co_3O_4 electrodes for Cl_2 evolution from N_2 saturated 4.5 mol dm^{-3} NaCl solutions with the temperature of preparation. • – *without* RuO_2 interlayer; ○ – *with* RuO_2 interlayer. $E = 1.1$ V (SCE).

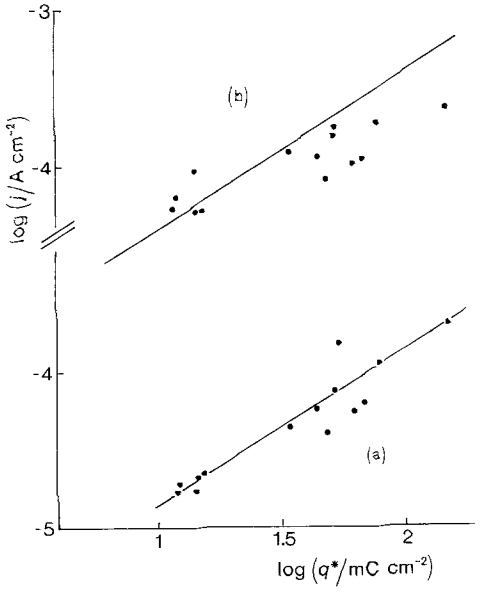

Fig. 13. Variation of the electrocatalytic activity of Co_3O_4 electrodes for Cl_2 evolution with the voltametric charge, q^*, in N_2 saturated (a) 4.5 and (b) 0.5 mol dm^{-3} NaCl solutions. $E = 1.1$ V (SCE). ——— – straight line of unit slope.

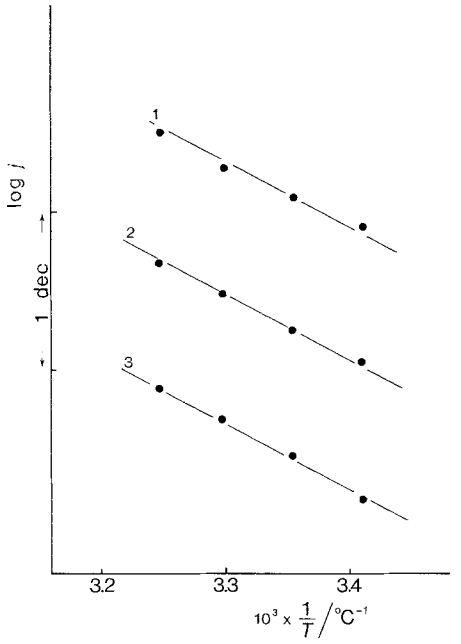

Fig. 14. Typical Arrhenius plots of the electrocatalytic activity for Cl_2 evolution as a function of reciprocal temperature for three Co_3O_4 electrodes in N_2 saturated 5 mol dm^{-3} NaCl solutions. 1. 260° C, with RuO_2 interlayer; 2. 300° C; 3. 500° C, with RuO_2 interlayer. E = 1.1 V (SCE).

of difficult quantitative interpretation because the energetic state of adsorbed intermediates is usually not known. $E^{\neq}$ is however very useful on a qualitative basis for comparison between different electrodes.

Fig. 14 shows a typical Arrhenius plot for the dependence of the activity of Co_3O_4 electrodes in Cl_2 evolution on temperature. The derived $E^{\neq}$ amounts to about 75 ± 4 kJ mol^{-1} and its dependence on q^* is shown in Fig. 15. If the points are analysed by the least squares method, some possible dependence on q^* shows up (see the dashed straight line). The total variation of q^* is *c.* 3 kJ mol^{-1} over a q^* range of *c.* 90 mC cm^{-2}. This amounts to about 4% of the total value of $E^{\neq}$ and is probably not very significant. On the other hand, as seen in Fig. 11, Cl_2 diffusion problems may become appreciable as q^* increases. Therefore, the small decrease of $E^{\neq}$ might be consistently understood in terms of a small diffusion component in the reaction rate.

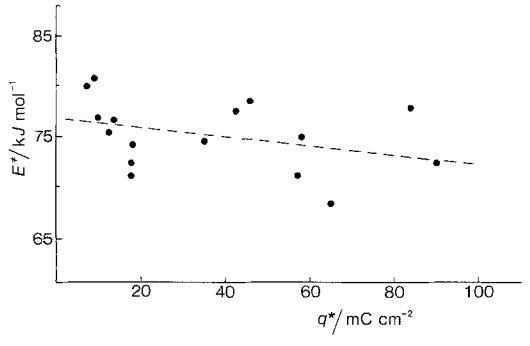

Fig. 15. Variation of the apparent activation energy for Cl_2 evolution on Co_3O_4 electrodes with the voltametric charge, q^*. N_2 saturated 5 mol dm^{-3} NaCl + 0.01 mol dm^{-3} HCl solutions. E = 1.1 V (SCE). – – – – – straight line calculated by the least squares method.

3.7. Reaction orders

Since the Tafel slope of 0.040 V may be consistent with a number of different mechanisms, the reaction order becomes the crucial factor to discriminate between the various possibilities. Much of the discussion that has arisen in the literature [28–31] about the mechanism of Cl_2 evolution at RuO_2 electrodes has been in fact centred on the most probable value of the reaction order with respect to Cl^-. In what follows, it is shown that a source of divergence between different authors is probably the unexpected and unpredictable effect of the solution pH.

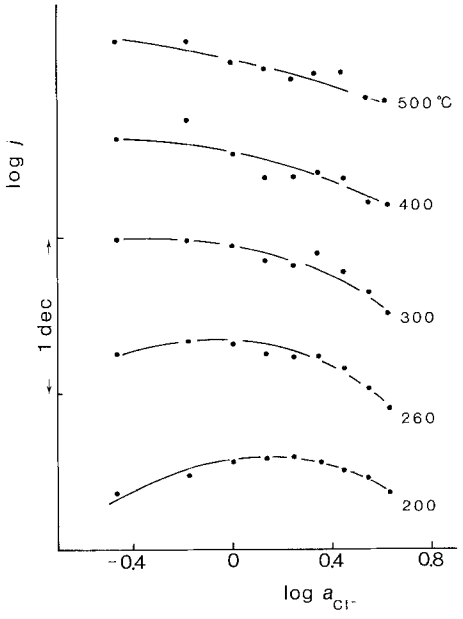

Fig. 16. Plot of the reaction rate for Cl_2 evolution at Co_3O_4 electrodes against the Cl^- activity at constant HCl concentration (0.01 mol dm^{-3}). E = 1.1 V (SCE).

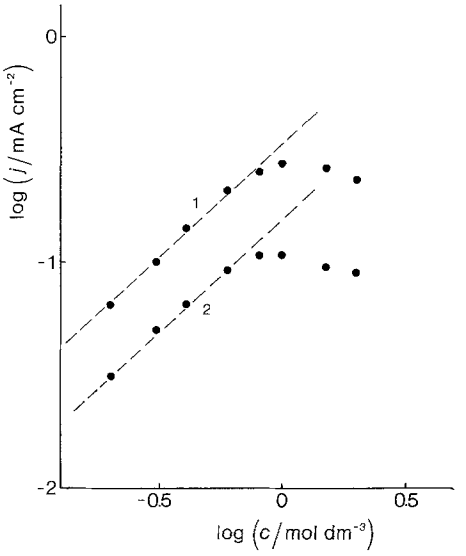

Fig. 17. Plot of the reaction rate for Cl_2 evolution at two Co_3O_4 electrodes against the Cl^- concentration in NaCl + 0.01 mol dm^{-3} HCl + 1 mol dm^{-3} $NaClO_4$ solutions. 1. 260° C; 2. 300° C, with RuO_2 interlayer. $E = 1.1$ V (saturated NaCl). – – – – – straight line of unit slope.

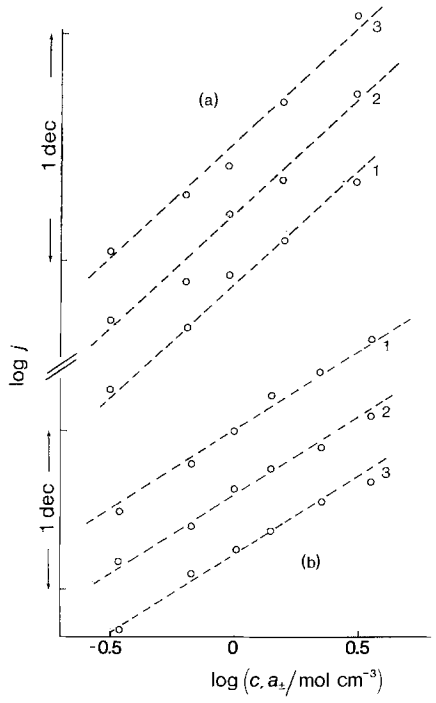

Fig. 18. Reaction rate for Cl_2 evolution at Co_3O_4 electrodes at variable Cl^- activity: (a) [$E = 1.1$ V (SCE)] and at variable Cl^- concentration in 1 mol dm^{-3} $NaClO_4$ solutions; (b) [$E = 1.15$ V (saturated NaCl)] at constant pH (*c.* 1). – – – – – straight line of unit slope. Conditions of preparation: 1a. 230° C with RuO_2; 2a. 400° C; 3a. 500° C with RuO_2; 1b. 230° C; 2b. 400° C with RuO_2; 3b. 500° C with RuO_2.

Fig. 16 shows the variation of the reaction rate of Cl_2 evolution with the Cl^- activity measured by simply changing the Cl^- concentration without any attention to the solution pH. The apparent reaction order is mainly negative, close to zero. For the most active electrodes it goes through a maximum at intermediate concentrations. Similar results for RuO_2 electrodes were earlier interpreted [32] in terms of self-inhibition of the anodic reaction due to Cl^- specific adsorption.

If the determination of the reaction order is carried out with a constant large concentration of inert electrolyte, Fig. 17 shows that a reaction order of 1 tending to zero as the Cl^- concentration is increased is observed. Similar results for RuO_2 electrodes were earlier interpreted [32] in terms of the screening effects of the electrode charge by the inert electrolyte and suppression of the Cl^- specific adsorption in the low Cl^- concentration range.

It is now clear that these results are due to the pH effects illustrated in Figs. 5 and 6. In particular, the smooth variation in shape of the curves in Fig. 16 is to be related to the combination of morphology and pH effects. More specifically, for the most active electrodes (low calcination temperature) the reaction rate is depressed at low Cl^- concentrations because of porosity effects (cf. Fig. 13) and at high Cl^- concentrations because of pH effects. Therefore, the apparent reaction rate goes through a maximum. As the value of q^* decreases, then the porosity decreases. As a result, the variation of the reaction rate is dominated by pH effects over the Cl^- concentration range and it decreases monotonically with a_{Cl^-} (cf. the electrode prepared at 500° C).

The role of the solution pH is quantitatively illustrated in Figs. 18 and 19. The variation of the reaction rate with the activity of Cl^- in solution *at constant pH* is shown in Fig. 18, Curve a. The reaction order with respect to Cl^- is 1 beyond any reasonable doubt. Fig. 18, Curve b, shows that the same result is obtained in the presence of an inert electrolyte at high concentration. Fig. 19 shows that, at constant Cl^- concentration, the reaction rate is depressed by a decrease in the solution pH. The order of reaction with respect to H^+ is therefore -1. The Tafel slope was not observed to depend on pH.

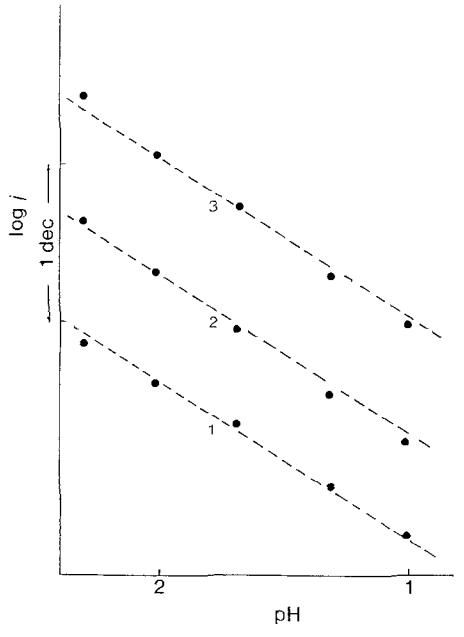

Fig. 19. Reaction rate at 1.1 V (SCE) for Cl_2 evolution at three Co_3O_4 electrodes from 1 mol dm^{-3} NaCl solutions as a function of the pH. – – – – – straight line of unit slope. 1. 230° C; 2. 300° C; 3. 400° C.

3.8. Reaction mechanism

Table 1 summarizes the kinetic parameters of the anodic Cl_2 evolution reaction at Co_3O_4 electrodes. These parameters do not depend on the procedure of preparation of the electrode. The standard rate constant is however strongly dependent on the temperature of calcination of the active layer. Results show that this dependence is related to the variation with temperature in the surface concentration of active sites which appears to be proportional to the extension of the surface area. The order of reaction with respect to the active sites is therefore 1 and no extra electrocatalytic effects are produced by a change in the calcination temperature.

Table 1. Summary of the kinetic parameters of the anodic evolution of chlorine at Co_3O_4 electrodes

Parameter	*Value*
Reaction order (η = const.)	
Cl^-	$(1-2\alpha)$
Cl_2	α
H^+	-1
Anodic transfer coefficient, α	*c.* 0.5
Stoichiometric number, ν	*c.* 1
Tafel slope	$RT/(1+\alpha)F$
Reaction order (E = const.)	
Cl_2	0
Cl^-	1
H^+	-1
(Surface sites)	(1)
Activation energy, E = 1.1 V (SCE)	*c.* 75 kJ mol^{-1}

The Tafel slope of 0.040 V suggests that the second electron transfer is probably rate determining. However, the reaction order of 1 with respect to Cl^- rules out the discharge of $2Cl^-$ in the rate determining step and in the preceding steps. Moreover, the effect of the pH indicates that oxidation of hydroxylic species must precede the Cl^- discharge. Therefore, electron transfer from Cl^- is thought to take place at an oxidized site. The metal cation is probably inaccessible to direct discharge of Cl^- because of coverage by water molecules and hydroxyl groups [13]. Since in the low pH range the surface of Co_3O_4 is positively charged, a possible mechanism is the following:

$$S\text{–}OH_2^+ + Cl^- \rightleftarrows S\text{–}OH_2Cl \qquad (7a)$$

$$S\text{–}OH_2Cl \rightleftarrows S\text{–}OHCl + H^+ + e \qquad (7b)$$

$$S\text{–}OHCl \rightarrow S\text{–}(OHCl)^+ + e \qquad \text{rds} \qquad (7c)$$

$$S\text{–}(OHCl)^+ + Cl^- + H^+ \rightleftarrows S\text{–}OH_2^+ + Cl_2 \qquad (7d)$$

where Reaction 7a expresses the electrostatic adsorption of negative ions onto positively charged sites.

The discharge of Cl^- directly onto the metal cation is probably difficult because it would involve the displacement of a hydroxyl group by the chloride whose negative charge would then lead to true retarding effects. These have however been ruled out. Therefore, in the mechanism shown in Equations 7a–d the Cl^- discharge is 'mediated' by the adsorbed OH group. This explains the role of the pH and also why no fractional reaction orders are observed, unlike the case of O_2 discharge [31, 33] which takes place at the bare cations of the oxide surface. The kinetic equation for the mechanism of Equations 7a–d is the following:

$$\eta = \ln 2Fk^0 - \frac{RT}{(1+\alpha)F}\ln a_{Cl^-} + \frac{RT}{(1+\alpha)F}\ln j + \frac{RT}{(1+\alpha)F}\ln a_{H^+} \qquad (8)$$

Table 2. Chronology of voltametric charge (q^*) determination runs

Run	*Description of the experiments*
1	Fresh electrodes (After)
2	O_2 evolution from KOH solution (Tafel line)
3	O_2 evolution: reaction order and activation energy Cl_2 reaction: reaction resistance at different a_{Cl^-} and different p_{Cl_2} (About one year interruption)
4	Cl_2 evolution from 5 mol dm^{-3} NaCl (Tafel line)
5	Cl_2 evolution: reaction order (Cl^-)
6	Cl_2 evolution from 1 mol dm^{-3} NaCl (Tafel line) Activation energy in 5 mol dm^{-3} NaCl
7	Cl_2 evolution: reaction resistance in 1 mol dm^{-3} NaCl
8	Cl_2 evolution from 1 mol dm^{-3} NaCl with Cl_2 (Tafel line)
9	Voltametric curves far from O_2 evolution in a narrow potential range to investigate surface area
10	Cl_2 evolution: reaction order (Cl^-) in the presence of inert electrolyte

The involvement of oxygenated species in the mechanism of Cl_2 evolution has been suggested several times for RuO_2 electrodes [27–29, 34]. However, the kinetic role of protons has never been pointed out except in the very recent work of Krishtalik *et al.* [17]. In particular, Harrison, Caldwell and White [35] have suggested that HClO may be involved as an electroactive species, but they failed to observe any pH effect in Cl_2 evolution at $TiO_2 + RuO_2$ electrodes [28]. Therefore, they have proposed [28] that water discharge follows (and does not precede) the Cl^- discharge, which is physically much more difficult to rationalize.

3.9. External surface stability

While no specific study of the anodic wear under high current density was carried out, the stability of the electrode was monitored by measuring the voltammetric charge q^* before and after each set of experiments. The chronological sequence of the experiments is detailed in Table 2.

Fig. 20 displays the variation of q^* in the course of the experiments. The vertical dashed line marks an interruption in the use of these electrodes for about one year. The general trend of q^* is to increase with use. This suggests that the surface probably undergoes a continuous wear (however small) that results in roughening. The increase in q^* is, however, not indefinite. After some runs, q^* decreases sharply or even collapses. This is presumably due to some mechanical 'polishing' of the surface resulting in removal of the smaller particles.

The general trend is also observed to depend on the temperature of preparation of the electrode, which points to the role of morphology. Fig. 21 shows the average behaviour of q^* as a function of the calcination temperature. Since an increase in q^* is paralleled by an increase in electrocatalytic activity, Fig. 21 shows that this

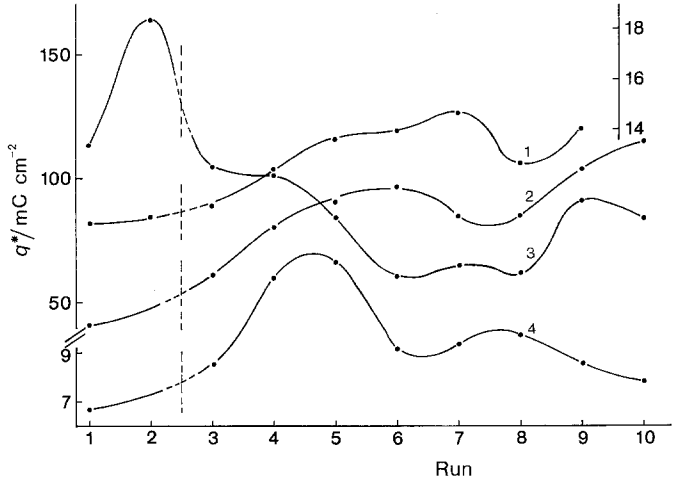

Fig. 20. Modification of the voltametric charge of Co_3O_4 electrodes in the course of the experiments, as described in Table 1. 1. 300° C, with RuO_2 interlayer; 2. 230° C, with RuO_2 interlayer; 3. 200° C; 4. 400° C. For the vertical dashed line, see text.

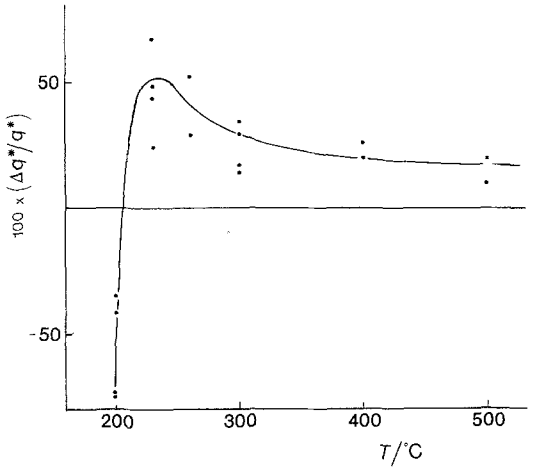

Fig. 21. Relative variation of the voltametric charge of Co_3O_4 electrodes between Point 2 and Point 3 in Fig. 20, as a function of the temperature of preparation.

beneficial effect is maximum at temperatures around 250° C. At 200° C the trend is towards a sharp decrease of q^* which indicates that the active layer is very disperse and poorly adherent. In the high temperature range, q^* tends to a moderate increase with a substantial stability of the surface morphology.

3.10. Inner interface stability

The value of q^* is not sensitive to modifications at the support–active layer interface unless a blocking effect occurs. Evidence for a deterioration of the ohmic contact between Ti and the overlayer is provided by the potential difference between the anodic and cathodic peaks of the voltametric curve in KOH. With fresh electrodes with a RuO_2 interlayer, the two peaks fall almost at the same potential. Fig. 22 shows that after the electrodes have been used in experiments the two peaks shift further apart. This might be related to the increased irreversibility of the adsorption–desorption reaction of oxygenated species but the distortion of the voltametric curve, and the features which will be illustrated below, lead us to think that the apparent decoupling of the peaks is probably related to the growth of an insulating layer at the Ti–oxide interface.

Fig. 23 illustrates the dependence of the peak separation on the calcination temperature and the presence or absence of the RuO_2 interlayer. Fresh

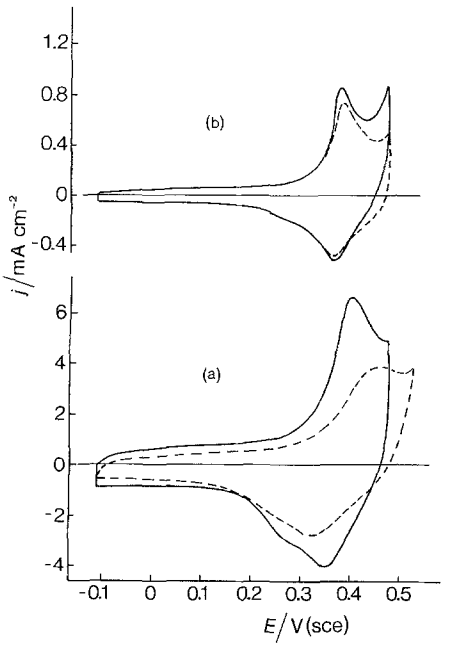

Fig. 22. Comparison of voltametric curves between Co_3O_4 electrodes ——— – with and – – – – – without RuO_2 interlayer in correspondence to Point 9 in Fig. 20: (a) 230° C; (b) 400° C.

electrodes with RuO_2 interlayer show no peak separation down to *c.* 260° C. At lower temperatures some peak separation appears also with RuO_2. This may be due to the fact that at the lowest temperature the oxide layer is constituted by poorly adherent (see above), extremely fine particles. Thus, the electrocatalyst does not protect the underlying Ti surface from contact

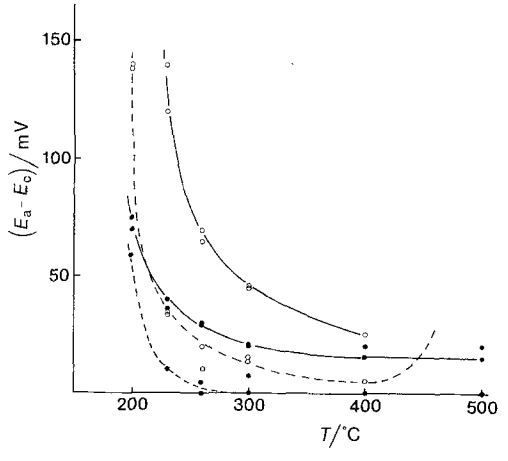

Fig. 23. Difference between anodic and cathodic peak potentials – – – – – for fresh Co_3O_4 and ——— for electrodes in correspondence to Point 4 in Fig. 20. Electrodes • – with and ○ – without RuO_2 interlayer.

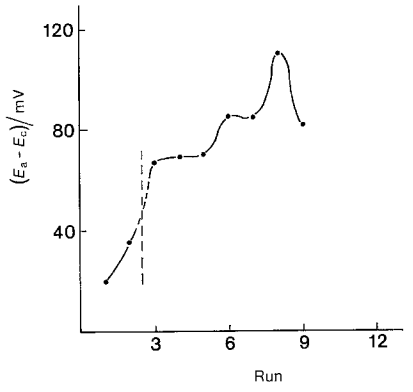

Fig. 24. Variation in the course of experiments, as described in Table 1, of the difference between anodic and cathodic peak potentials for a Co_3O_4 electrode prepared at 260° C without RuO_2 interlayer.

with the solution in the cell and the oxygenated atmosphere outside the cell. Moreover, lattice constituents are presumably very mobile in the presence of a large number of defects. In the absence of the RuO_2 interlayer, fresh electrodes exhibit peak separation at any calcination temperature. After some use, the peak separation increases. The increase is minimum for electrodes with the RuO_2 interlayer prepared at temperatures between 300 and 500° C.

Fig. 24 illustrates, for one specific electrode, the variation of the peak separation in the course of the experiments. It is interesting that polarization during O_2 evolution or Cl_2 evolution from diluted brines enhances the peak separation. Polarization in concentrated brine, on the contrary, does not produce any appreciable change in q^*. Therefore, the occurrence of water or OH^- discharge seems to be responsible for the change in q^*. Since O_2 evolution leads to some ordering in the Co_3O_4 lattice with shift of the composition towards stoichiometry [36], the peak separation might also be related to modifications in the structure of the oxide surfaces. The decrease in q^* in Fig. 24 in fact took place after some experiments where no oxygen was evolved and the potential was mainly kept far from the anodic limit. In this case, however, the peak separation should be visible also with fresh electrodes and should be a function of the calcination temperature, since stoichiometry increases as the temperature is raised.

The alternative possibility is that only during oxygen evolution can oxygenated species reach the Ti surface where the insulating layer can grow and this is easier with defective, poorly crystalline, finely dispersed electrocatalysts. On the other hand, the peak separation with fresh electrodes without RuO_2 is very likely to be due to the presence of the TiO_2 insulating layer. Thus, the two mechanisms might be both operative, but the latter should largely prevail.

4. Conclusions

Co_3O_4 exhibits an interesting activity for the anodic evolution of Cl_2. Although RuO_2 is intrinsically more active, the difference is small enough to make the replacement of the precious metal oxide economically favourable. However, long-term performances have not been investigated specifically.

The activity of Co_3O_4 electrodes depends on the temperature of their preparation. It increases exponentially with decreasing temperature below 300° C but the stability of the active layer becomes poorer. At temperatures higher than 400° C the oxide layer is very stable but its activity is low because of excessive crystallization and sintering.

Problems arise at the oxide–Ti interface. During the calcination, a TiO_2 film is formed. Its effect can be minimized by interposing a thin layer of RuO_2. Without this layer, no electrode can be prepared at temperatures higher than 400° C. In the lower temperature range the insulating layer may form during anodic polarization because the active oxide is poorly crystalline and non-protective. Low-temperature layers deteriorate mechanically rather easily upon use.

Anodic Cl_2 evolution at Co_3O_4 electrodes is kinetically controlled by the interfacial transfer of the second electron. The first electron is, however, not exchanged with a Cl^- ion but with an adsorbed oxygenated species which thus releases a proton. This step is responsible for the observed pH dependence of the reaction rate which is thermodynamically unpredictable. In particular, the anodic reaction rate is depressed by an increase in the acidity of the solution. This unexpected kinetic feature of Cl_2 evolution at oxide electrodes is very likely to be the origin of the discrepancies between the results of different authors and for

the consequent long debate about the mechanism of the anodic reaction.

Acknowledgements

Financial support to this work by the Italian National Research Council (CNR, Rome) is gratefully acknowledged. A.C. is indebted to O. De Nora S.p.A., Milan, for a fellowship during which part of this work was carried out.

Note added in proof

With this paper already submitted for publication, Dr R. G. Erenburg has drawn the authors' attention to a paper in Dvoinoi Sloi i Adsorbtziyana Tverdykh Elektrodakh, Vol 6, Tartus. Gos. Univ., 1981, pp. 382–5 (in Russian) where a mechanism similar to that proposed in this paper was first postulated.

References

[1] D. L. Caldwell and M. J. Hazelrigg, in 'Modern Chlorine Alkali Technology', (edited by M. O. Coulter) Ellis Horwood, Chichester (1980) pp. 121–135.
[2] A. Tvarusko, 34th ISE Meeting, Erlangen, 19–23 September 1983. Extended Abstract III–7.
[3] M. B. Konovalov, V. I. Bystrov and V. L. Kubasov, *Elektrokhim.* **12** (1976) 1266.
[4] R. A. Agapova and G. N. Kokhanov, *ibid.* **12** (1976) 1649.
[5] D. M. Shub, M. F. Reznik, V. V. Shamaginov, E. N. Lubnin, N. V. Kozlova and V. N. Lomova, *ibid.* **19** (1983) 502.
[6] V. V. Shalaginov, D. M. Shub, N. V. Kozlova and V. N. Lomova, *ibid.* **19** (1983) 537.
[7] M. R. Tarasevich and B. N. Efremov, in 'Electrodes of Conductive Metallic Oxides'. Part A (edited by S. Trasatti) Elsevier, Amsterdam (1980) pp. 221–259.
[8] R. Garavaglia, C. M. Mari, S. Trasatti and C. De Asmundis, *Surf. Technol.* **19** (1983) 197.
[9] G. Lodi, E. Sivieri, A. De Battisti and S. Trasatti, *J. Appl. Electrochem.* **8** (1978) 135.
[10] A. Carugati and S. Trasatti, in preparation.
[11] C. M. Mari, R. Garavaglia, A. Carugati and S. Trasatti, 31st ISE Meeting, Venice, 1980. Extended Abstracts, p. 49.
[12] B. N. Efremov and M. R. Tarasevich, *Elektrokhim.* **17** (1981) 1672.
[13] A. Daghetti, G. Lodi and S. Trasatti, *Mater. Chem. Phys.* **8** (1983) 1.
[14] R. Parsons, 'Handbook of Electrochemical Constants', Butterworths, London (1959).
[15] D. M. Shub, A. N. Chemodanov and V. V. Shalaginov, *Elektrokhim.* **14** (1978) 595.
[16] M. Spasojevic, N. Krstajic and M. Jaksic, *Surf. Technol.* **21** (1984) 19.
[17] L. I. Krishtalik, R. G. Erenburg, D. V. Kokoulina and R. I. Mostkova, 34th ISE Meeting, Erlangen, 19–23 September 1983. Extended Abstract III–6.
[18] B. V. Tilak, *J. Electrochem. Soc.* **126** (1979) 1343.
[19] M. Valigi and D. Gazzoli, in 'Solid State Chemistry 1982', Elsevier, Amsterdam (1983) pp. 197–200.
[20] S. Ardizzone, A. Carugati, G. Lodi and S. Trasatti, *J. Electrochem. Soc.* **129** (1982) 1689.
[21] V. V. Losev, *Elektrokhim.* **17** (1981) 733.
[22] L. J. J. Janssen, G. J. Visser and E. Barendrecht, *Electrochim. Acta* **28** (1983) 155.
[23] V. V. Shalaginov, I. D. Belova, Y. E. Roginskaya and D. M. Shub, *Elektrokhim.* **14** (1978) 1708.
[24] W. K. Rudlof and E. S. Freeman, Proceedings of the 7th International Conference on Thermal Analysis **1** (1982) 667.
[25] I. D. Belova, V. V. Shalaginov, B. S. Galyamov, Y. E. Roginskaya and D. M. Shub, *Zh. Neorg. Khim.* **23** (1978) 286.
[26] S. Trasatti, *Electrochim. Acta* **29** (1984) 1503.
[27] L. D. Burke and J. F. O'Neill, *J. Electroanal. Chem.* **101** (1979) 341.
[28] D. A. Denton, J. A. Harrison and R. I. Knowles, *Electrochim. Acta* **24** (1979) 521.
[29] T. Arikado, C. Iwakura and H. Tamura, *ibid.* **23** (1978) 9.
[29] L. J. J. Janssen, L. M. C. Starmans, J. C. Visser and E. Barendrecht, *ibid.* **22** (1977) 1093.
[31] L. I. Krishtalik, *ibid.* **26** (1981) 329.
[32] R. G. Erenburg, L. I. Krishtalik and I. P. Yarosheskaya, *Elektrokhim.* **11** (1975) 1072.
[33] A. Carugati, G. Lodi and S. Trasatti, *Mater. Chem.* **6** (1981) 255.
[34] J. Augustynski, L. Balsenc and J. Hinden, *J. Electrochem. Soc.* **125** (1978) 1093.
[35] J. A. Harrison, D. L. Caldwell and R. E. White, *Electrochim. Acta* **28** (1983) 1561.
[36] B. N. Efremov, G. I. Zakharkin, S. R. Zhukov and M. R. Tarasevich, *Elektrokhim.* **14** (1978) 937.